



FULL LENGTH ARTICLE

# Single-cell transcriptome landscape and antigen receptor dynamic during SARS-CoV-2 vaccination

Xiaojian Cao <sup>a,1</sup>, Xiaohua Chen <sup>b,\*\*\*,1</sup>, Yaqi Zhu <sup>d</sup>, Xiaojuan Gou <sup>a</sup>, Keyi Yan <sup>f</sup>, Bing Yang <sup>a</sup>, Dong Men <sup>g</sup>, Lei Liu <sup>h</sup>, Yong-an Zhang <sup>e,\*\*\*</sup>, Gang Cao <sup>a,c,\*</sup>



<sup>a</sup> State Key Laboratory of Agricultural Microbiology, College of Veterinary Medicine, Huazhong Agricultural University, Wuhan, Hubei 430072, China

<sup>b</sup> Department of Laboratory Medicine, Nanfang Hospital, Southern Medical University, Guangzhou, Guangdong 51015, China

<sup>c</sup> Bio-Medical College, Huazhong Agricultural University, Wuhan, Hubei 430072, China

<sup>d</sup> Department of Laboratory Medicine, Maternal and Child Health Hospital of Hubei Province, Wuhan, Hubei 430070, China

<sup>e</sup> State Key Laboratory of Agricultural Microbiology, College of Fisheries, Huazhong Agricultural University, Wuhan, Hubei 430072, China

<sup>f</sup> Spatial FISH Co. Ltd., Jiangmen, Hubei 529199, China

<sup>g</sup> State Key Laboratory of Virology, Wuhan Institute of Virology, Center for Biosafety Mega-Science, Chinese Academy of Sciences, Wuhan, Hubei 430071, China

<sup>h</sup> Department of Transfusion Medicine, General Hospital of Central Theater Command, PLA, Wuhan, Hubei 430070, China

Received 18 April 2022; received in revised form 4 August 2022; accepted 12 August 2022

Available online 8 September 2022

## KEYWORDS

COVID-19;  
SARS-CoV-2;

**Abstract** Vaccination by inactivated vaccine is an effective strategy to prevent the COVID-19 pandemic. However, the detailed molecular immune response at single-cell level is poorly understood. In this study, we systematically delineated the landscape of the pre- and post-

\* Corresponding author. State Key Laboratory of Agricultural Microbiology, College of Veterinary Medicine, Huazhong Agricultural University, Wuhan, Hubei 430072, China.

\*\* Corresponding author. Department of Laboratory Medicine, Nanfang Hospital, Southern Medical University, Guangzhou 51015, China.

\*\*\* Corresponding author. State Key Laboratory of Agricultural Microbiology, College of Fisheries, Huazhong Agricultural University, Wuhan 430072, China.

E-mail addresses: [chenxiao@whu.edu.cn](mailto:chenxiao@whu.edu.cn) (X. Chen), [yonganzhang@mail.hzau.edu.cn](mailto:yonganzhang@mail.hzau.edu.cn) (Y.-a. Zhang), [gcao@webmail.hzau.edu.cn](mailto:gcao@webmail.hzau.edu.cn) (G. Cao).

Peer review under responsibility of Chongqing Medical University.

<sup>1</sup> These authors contributed equally.

Single-cell sequencing;  
TCR sequencing;  
Vaccination

vaccination single-cell transcriptome, TCR (T cell antigen receptor) and BCR (B cell antigen receptor) expression profile of vaccinated candidates. The bulk TCR sequencing analysis of COVID-19 patients was also performed. Enrichment of a clonal CD8<sup>+</sup> T cell cluster expressing specific TCR was identified in both vaccination candidates and COVID-19 patients. These clonal CD8<sup>+</sup> T cells showed high expression of cytotoxicity, phagosome and antigen presentation related genes. The cell–cell interaction analysis revealed that monocytes and dendritic cells could interact with these cells and initiate phagocytosis via ICAM1-ITGAM and ITGB2 signaling. Together, our study systematically deciphered the detailed immunological response during SARS-CoV-2 vaccination and infection. It may facilitate understanding the immune response and the T-cell therapy against COVID-19.

© 2022 The Authors. Publishing services by Elsevier B.V. on behalf of KeAi Communications Co., Ltd. This is an open access article under the CC BY-NC-ND license (<http://creativecommons.org/licenses/by-nc-nd/4.0/>).

## Introduction

Corona Virus Disease 2019 (COVID-19) posed a severe threat to public health. While extensive vaccination is an effective strategy to prevent the COVID-19 pandemic, the detailed molecular immune response is poorly understood. It has been well characterized that neutralizing antibodies secreted by B cells can prevent severe acute respiratory coronavirus-2 (SARS-CoV-2) binding to angiotensin-converting enzyme 2 (ACE2) on epithelial cells.<sup>1,2</sup> While the single-cell analysis has been performed with COVID-19 patients,<sup>3–5</sup> the T cell response and repertoire dynamic after vaccination and infection, especially at the single-cell level, remains elusive. It has been shown that the duration of immunologic memory of T cells is longer than B cells.<sup>6</sup> Moreover, CD4<sup>+</sup> T cells can facilitate antibody production by B cells and CD8<sup>+</sup> T cells can eliminate the infected cells to restrict virus proliferation.<sup>7</sup> Thus, systematic illumination of the detailed T cells response during SARS-CoV-2 infection and vaccination would be of great importance to the understanding of the host defense mechanism against SARS-CoV-2.

T cell antigen receptors (TCRs) are immunoglobulin-like molecules composed of the variable (V), diversity (D), join (J) and constant (C) regions.<sup>8</sup> The specificity of the recognition depends on the specific selection of the variable and join gene segments during the rearrangement of TCR genes.<sup>9</sup> The enrichment and selection of pathogen-specific TCR-carrying T cells during maturation and differentiation play a crucial role in adaptive immunity. The junction of germline V, D, J and C regions forms the complementarity determining region 3 (CDR3) region, which possesses the highest variability in both  $\alpha/\beta$  or  $\gamma/\delta$  chains of TCR. The structure of the CDR3 region determines the binding affinity of TCR to the epitope-MHC complex.<sup>10</sup> Due to the specificity of TCR corresponding to the pathogen, the TCR clonotype spectrum can reflect the immune status of individuals<sup>11</sup> and reflect the infection of a certain disease. Moreover, as CAR-T-based therapy has been applied to many virus infectious diseases including AIDS, EBV, HBV and HCV,<sup>12</sup> the identification of this TCR clonotype may facilitate the chimeric antigen receptor T cell (CAR-T) therapy for COVID-19. The integrated analysis of single-cell

transcriptome and vdj sequencing facilitates the identification of the unraveled function of T cells, leading to further understanding of the immune system.

This study aims to systematically delineate the landscape of the molecular events of immunological response, especially T cells response during vaccination and SARS-CoV-2 infection, by using single-cell transcriptome and single-cell TCR/BCR analysis.

## Methods

### Design of the study

As shown in Figure 1A, human peripheral blood lymphocyte was isolated from 2 vaccine candidates at 3 days pre 1st vaccination, and 15 days post 2nd vaccination. Patients' and healthy controls' blood samples were also isolated. Lymphocytes from vaccine candidates were subjected to the single-cell transcriptome, TCR and BCR library construction. Lymphocytes from patients and healthy control were subjected to bulk TCR library construction.

### Human project

Ninety-four blood donors were involved in the study, including dead COVID-19 patients ( $n = 6$ ), convalescent COVID-19 patients ( $n = 50$ ), healthy control ( $n = 36$ ), and inactivated SARS-CoV-2 vaccination candidates ( $n = 2$ ) with vaccine which was provided by Wuhan Institute of Biological Product (Wuhan, China), produced by infection of SARS-CoV-2 WIV04 strain in Vero cell, and contains 0.5 mL with 200WU SARS-CoV-2 antigen in a single dose. Lymphocytes were isolated from blood contained in EDTA-K<sub>2</sub> tubes by a human peripheral blood lymphocyte isolation kit (TBD, China) following the manufacturer's instructions. Lymphocytes for bulk TCR/BCR sequencing were directly resuspended into TRIzol reagent (Invitrogen, USA), while samples for 10X library construction were resuspended in RPMI supplemented with 20% dimethyl sulfoxide (Thermo, USA) and 60% fetal bovine serum (Gibco, USA) and stored in liquid nitrogen.

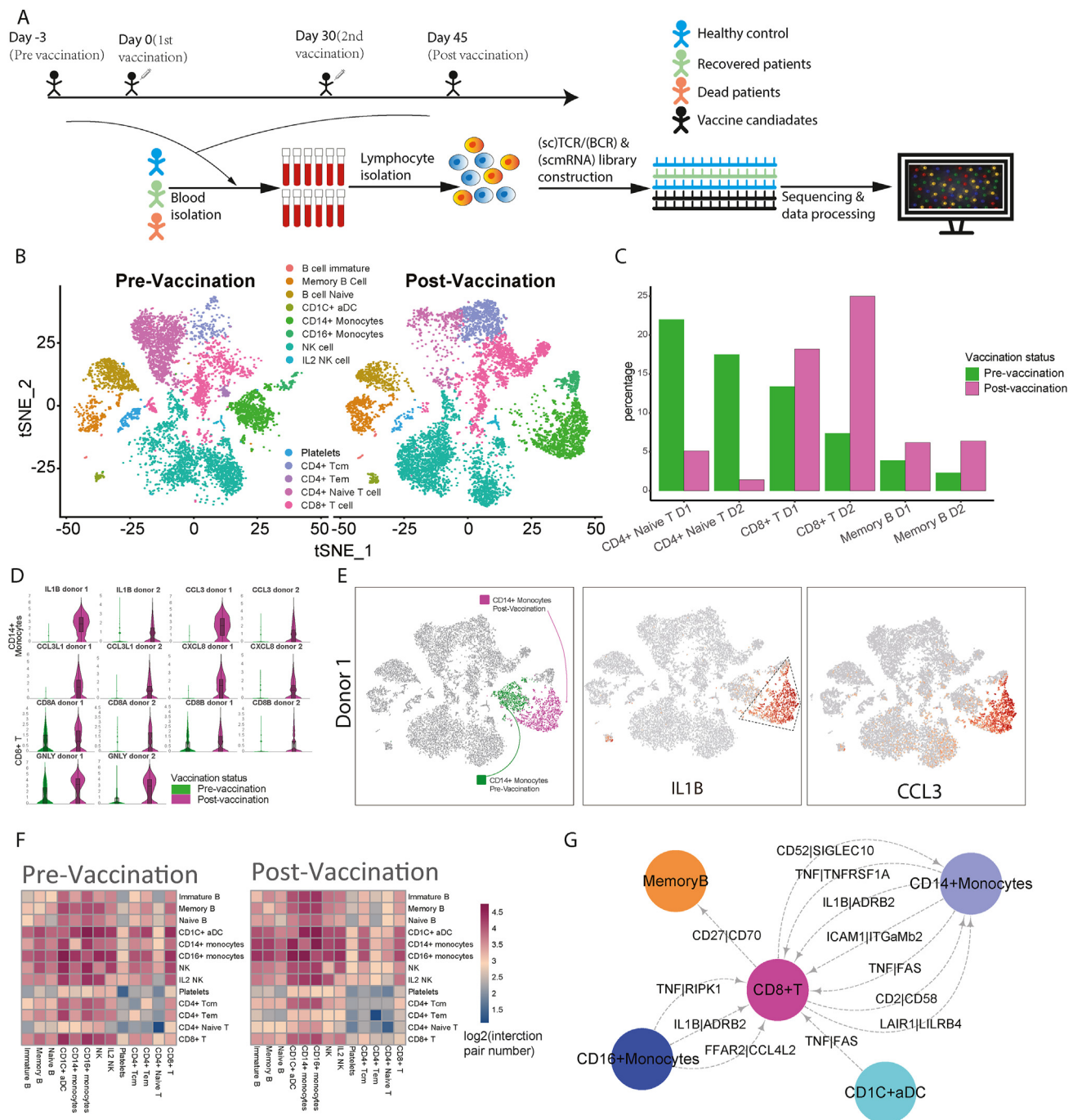


**Figure 1** Single cell transcriptome profiling of the vaccination candidates. **(A)** Design of the study. **(B)** tSNE plot of Donor 1 pre-vaccination and post-vaccination. **(C)** Bar chart showing the percentage of different types of cells in Donor 1 and Donor 2 pre-vaccination and post-vaccination. **(D)** Violon plot illustrating the expression of *IL1B*, *CCL3*, *CCL3L1* and *CXCL8* in CD14<sup>+</sup> monocytes, *CD8A*, *CD8B* and *GNLY* in CD8<sup>+</sup> T cells of Donor 1 and Donor 2. **(E)** IL-1B and IL1RN projection on the tSNE map of Donor 1 and Donor 2, the orange filled dots indicate intermediate expression level, while the red indicates high expression level. **(F)** Heatmap showing the cell-cell interaction probability among different cell types of Donor 1 and Donor 2, with red color indicates high probability, with blue indicating low probability. **(G)** CD8<sup>+</sup> T cells centered interaction network in both Donor 1 and Donor 2 post-vaccination with the molecular pairs in ligand (source cell) in left and receptor (target cell) in right. These interactions cannot be detected pre-vaccination.

## RNA isolation and library construction

RNA isolation was conducted with standard TRIzol protocol (Invitrogen, USA). Bulk TCR and BCR libraries were constructed by template switch and nested PCR-based protocol. Briefly, total RNA was reverse transcribed with SMARTscribe (Takara, Japan) following the manufacturer's instructions using C-region specific primer corresponding to TRAC and TRBC. 2  $\mu$ L out of 10  $\mu$ L solved cDNA was applied as the template for the 1st nested PCR KAPA Hot Start Ready Mix (KAPA, USA) following the manufacturer's instructions. 2nd and 3rd nested PCR were conducted with Phanta Max high fidelity polymerase (Vazyme, China), while the Illumina adapters were added to the fragments in the 3rd nested PCR. Beads-based purification was conducted after the 1st and the 2nd nested PCR and the final library was purified with cycle pure kit (Omega, USA). Single-cell mRNA, TCR, BCR libraries were constructed on 10X platform following the manufacturer's instructions. The DNA library was sequenced on Nova 2000 platform (Illumina, USA) under PE150 protocol.

## Bulk TCR data processing

The alignment and assembling of TCR clonotypes were conducted with MiXCR.<sup>13</sup> MiXCR result corresponding to every sample was first imported into R package immunarch (<https://CRAN.R-project.org/package=immunarch>) using RepLoad function. Then group based unique clonotypes were quantified using repExplore function under the "volume" function. The gene usage matrix demonstrating the frequency of each clonotype corresponding to every sample was outputted, student *t*-test and the median number of frequencies of each clonotype were pair wisely analyzed between every two groups. Clonotypes with significantly different expression frequencies (*P*-value < 0.05) between groups were selected and sorted by the ratio of the median of 2 groups. Box plot were used for the visualization of the data by inbuilt "vis" function of immunarch.

## 10X single-cell NGS data pre-processing

5' single-cell mRNA sequence data were first aligned and counted with function "count" of cellranger, then aggregate using the "aggr" function by the molecular information file in the output of count function. The count, barcode and feature matrix corresponding to every donor was imported into R package Seurat<sup>14</sup> and merged using the "merge" function. The mitochondrial transcripts, mRNA features and mRNA of every barcode (cell) were first quantified and the cells with >25 mitochondrial transcripts or mRNA features <200 or >4,000 were removed. The count was then normalized and clustering was conducted with "FindCluster" function under the resolution of 1.0. The clustering result was then subjected to R package SingleR<sup>15</sup> for cluster annotation.

## In-silico docking analysis

To compare the binding affinity of virus peptides with various TCR clonotypes, the interactive conformations of

SARS-CoV-2 nucleocapsid peptide N105-113 in complex with TRAV23-DV6-TRAJ52, TRBV7-6-TRBJ2-1, TRAV3-TRAJ17 and TRBV13- TRBJ2-3 were determined by Discovery Studio 2018 software. The X-ray structure of SARS-CoV-2 nucleocapsid peptide N105-113 was downloaded from RCSB Protein Data Bank (<https://www.rcsb.org>, PDB code: 7LGD). The receptor and other redundant ligand structures were deleted using the Hierarchy View. TRAV sequences were downloaded from NCBI and the homology model was created by the online modeling software SWISS-MODEL (<https://swissmodel.expasy.org/>). Firstly, the created proteins were prepared by Clean Protein tools to remove the alternative conformations and to patch the missing side-chain atoms. Then, the proteins and prepared N105-113 peptide were inserted into the same Graphics View, and selected as receptor and ligand, respectively. The docking parameters were set as the following: Angular Step Size was calculated as a defined value 15, RMSD Cutoff was defined as 6.0, Interface Cutoff was defined as 9.0, Maximum Number of Clusters was defined as 50, and other parameters were defined as default. Finally, the docked conformations were optimized and re-scored using Refine Docked Protein tools. The docked protein complexes were analyzed and visualized by Analyze Protein Interface function, and the binding affinity between TCR clonotypes and virus peptides was estimated by Z-dock Score. Meanwhile, the structure illustrations were generated with this software.

## Data visualization

tSNE plot was conducted by "dimplot" function of package Seurat, tSNE projection table and barcode-cluster were exported and imported to the aggregated loupe file for the gene expression mapping on the tSNE map. Heatmap demonstrating markers of clusters was generated using Seurat.<sup>14</sup> Heatmap indicating the intensity of cell–cell interaction was generated using CellPhoneDB.<sup>16</sup> Heatmap showing the gene expression level, gene usage and fold-change were generated using TBtools.<sup>17</sup> Alluvial plot of TCR gene usage was generated using R package ggalluvial. Boxplot showing the distribution of gene usage ratio among groups was generated using ggplot2 (<https://ggplot2.tidyverse.org>). KEGG pathway enrichment and map mapping were conducted using R package ClusterProfiler<sup>18</sup> and pathview.<sup>19</sup> Interaction network visualization was conducted by Cytoscape.<sup>20</sup> Volcano plot was generated by R package ggplot2 and ggrepel (<https://CRAN.R-project.org/package=ggrepel>).

## Oligos in the bulk TCR library construction

The sequences of oligos are shown in Table 1.

## Statistics

The *P*-value of gene usage in bulk TCR sequencing was calculated by wilcox test, all the clonotype displayed in Figure 4 is a statistical difference in the comparison with *P*-value < 0.05.

**Table 1** Oligos used in the bulk-TCR library construction.

| Oligo_name             | Sequence  |
|------------------------|---|
| <i>Switch_adapter</i>  | AAGCAGTGGTATCAACGCAGAGTACTCTT(rG)5                      |
| <i>TRAC_RT_R</i>       | ACACATCAGAACATCCTTACTTTG                                |
| <i>TRBC_RT_R</i>       | CAGTATCTGGAGTCATTGA                                     |
| <i>SMART20_F</i>       | CACTCTATCCGACAAGCAGTGGTATCACCGCAG                       |
| <i>TRAC_1ST_nest_R</i> | TACACGGCAGGGTCAGGGT                                     |
| <i>TRBC_1ST_nest_R</i> | TGCTTCTGATGGCTCAAACAC                                   |
| <i>P5_2nd_nest_F</i>   | TCGTCGGCAGCGTC AGATGTGTATAAGAGACAG CACTCTATCCGACAAGCAGT |
| <i>TRAC_2nd_nest_R</i> | GTCTCGTGGGCTCGGAGATGTATAAGAGACAG GGGTCAGGGTTCTGGATAT    |
| <i>TRBC_2nd_nest_R</i> | GTCTCGTGGGCTCGG AGATGTGTATAAGAGACAG ACACSTTKTTCAAGGTCTC |
| <i>N701</i>            | CAAGCAGAAAGACGGCATAACGAGATTGCCTTAGTCTCGTGGGCTCGG        |
| <i>N702</i>            | CAAGCAGAAAGACGGCATAACGAGATCTAGTACGGTCTCGTGGGCTCGG       |
| <i>N703</i>            | CAAGCAGAAAGACGGCATAACGAGATTCTGCCTGTCCTCGTGGGCTCGG       |
| <i>N704</i>            | CAAGCAGAAAGACGGCATAACGAGATGCTCAGGAGTCTCGTGGGCTCGG       |
| <i>N705</i>            | CAAGCAGAAAGACGGCATAACGAGATAGGAGTCCGTCCTCGTGGGCTCGG      |
| <i>N706</i>            | CAAGCAGAAAGACGGCATAACGAGATCATGCCATTCTCGTGGGCTCGG        |
| <i>N707</i>            | CAAGCAGAAAGACGGCATAACGAGATGTAGAGAGGTCTCGTGGGCTCGG       |
| <i>N708</i>            | CAAGCAGAAAGACGGCATAACGAGATCCTCTCGTGTCTCGTGGGCTCGG       |
| <i>N709</i>            | CAAGCAGAAAGACGGCATAACGAGATAGCGTAGCGTCCTCGTGGGCTCGG      |
| <i>N7010</i>           | CAAGCAGAAAGACGGCATAACGAGATCATGCCATTCTCGTGGGCTCGG        |
| <i>N7011</i>           | CAAGCAGAAAGACGGCATAACGAGATTGCCTTCTCGTGTCTCGTGGGCTCGG    |
| <i>N7012</i>           | CAAGCAGAAAGACGGCATAACGAGATCCTCTACGTCTCGTGGGCTCGG        |
| <i>N501</i>            | AATGATACGGCACCACCGAGATCTACACTAGATCGCTCGGCAAGCGTC        |
| <i>N502</i>            | AATGATACGGCACCACCGAGATCTACACCTCTATTCTCGTGGCAGCGTC       |
| <i>N503</i>            | AATGATACGGCACCACCGAGATCTACACTATCCTCTCGTGGCAGCGTC        |
| <i>N504</i>            | AATGATACGGCACCACCGAGATCTACAGAGTAGATCGTGGCAGCGTC         |
| <i>N505</i>            | AATGATACGGCACCACCGAGATCTACACTCGTGGCAGCGTC               |
| <i>N506</i>            | AATGATACGGCACCACCGAGATCTACACAAGAGTAGATCGTGGCAGCGTC      |
| <i>N507</i>            | AATGATACGGCACCACCGAGATCTACACAAGAGTAGATCGTGGCAGCGTC      |
| <i>N508</i>            | AATGATACGGCACCACCGAGATCTACACCTAAGCCTCGTGGCAGCGTC        |

## Results

### Single-cell transcriptome profiling of the SARS-CoV-2 vaccination candidates

To decipher the detailed immunological response during inactivated SARS-CoV-2 vaccination, we collected 4 blood samples from two candidates (Donor 1/Donor 2) 3 days before vaccination (pre-vaccination) and 15 days after the second dose of inactivated SARS-CoV-2 vaccination (post-vaccination) for single-cell transcriptome and single-cell TCR/BCR analysis (Fig. 1A). After the initial raw data filter, 41,391 cells were obtained including 12,611 cells from Donor 1, 8021 cells from Donor 2 pre-vaccination, 11,353 cells from Donor 1 and 9,406 cells from Donor 2 post-vaccination. These cells were classified into CD8<sup>+</sup> T cells, CD4<sup>+</sup> naïve T cells, CD4<sup>+</sup> central memory T cells (CD4<sup>+</sup> Tcm), naïve B cells, memory B cells, NK cells, IL2<sup>+</sup> NK cells, CD14<sup>+</sup> monocytes, CD16<sup>+</sup> monocytes, CD1C<sup>+</sup> aDC (a non-inflammatory CD1C<sup>+</sup> dendritic cell with high expression of type-II HLA comparing to inflammatory CD1C<sup>+</sup> dendritic cell CD1C<sup>+</sup> bDC, which facilitates strong antigen presentation) and CD34<sup>-</sup> pre-B cell by unbiased clustering analysis and annotated using singleR (Fig. 1B; Fig. S1A–C).

After vaccination, a higher percentage of CD8<sup>+</sup> T cells, Tcm, memory B cells in total peripheral blood

mononuclear cells (PBMCs) were observed in both vaccination donors (Fig. 1C; Fig. 1D, E). The comparison of gene expression in each cell type revealed a significantly higher expression level of *IL1B*, *CCL3*, *CCL3L1* and *CXCL8* in CD14<sup>+</sup> monocytes, and a higher expression level of *GNLY*, *CD8A* and *CD8B* in CD8<sup>+</sup> T cell after vaccination compared to that of pre-vaccination samples. Meanwhile, *CCL3L1*, *CXCL8* and *IL-1B* displayed a different level of up-regulation in CD14<sup>+</sup> monocytes after vaccination in comparison to that of the pre-vaccination (Fig. 1D, E; Fig. S3A). Moreover, up-regulation of *JUN* and *TNF* in CD14<sup>+</sup> monocytes, CD16<sup>+</sup> monocytes and CD1C<sup>+</sup> aDC cells post-vaccination (Fig. S2A–C); *IL10RA* and *IL6R* in CD4<sup>+</sup> Naïve T cells (Fig. S2D); *SELL* (CD62L), *CCR7* and *PTPRC* (CD45R) in CD4<sup>+</sup> Tcm (Fig. S2E); *JUN*, *FOSB*, *TRAV23-DV6* and *TRBV7-6* in CD8<sup>+</sup> T cells (Fig. S2F); *GNLY* and *IL10RA* in NK cells (Fig. S2G); *IFI30* and *IL3RA* in naïve B cell (Fig. S2H), *JUN* and *TNF* in memory B cells (Fig. S2I) were observed post-vaccination. Together, these data showed that the gene profiles of immunocytes underwent a dynamic change and were systematically activated post-vaccination.

To investigate the cell interaction network, the expression of genes encoding secreted protein genes and the corresponding receptor genes in each type of the cell were analyzed by cellphonedb. Distinct cell interaction patterns were observed among different cell types in pre- and post-vaccination groups (Fig. 1F; Fig. S1F). For

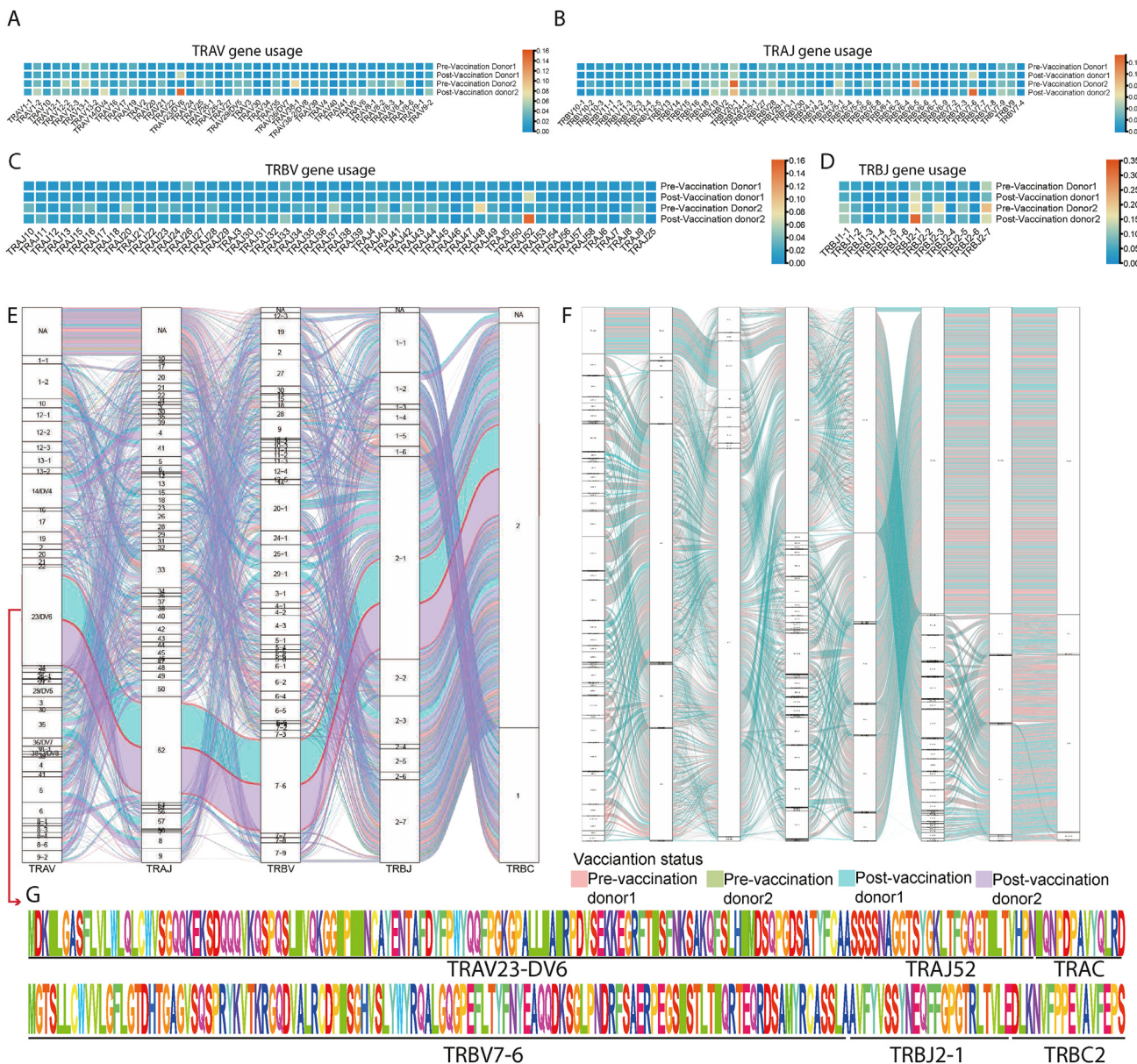


**Figure 2** TCR gene enrichment post-vaccination. **(A–D)** Heatmap of gene enrichment ratio corresponding to TRAV, TRAJ, TRBV and TRBJ region. **(E)** Alluvial plot showing the paired chain TCR gene enrichment of CD8<sup>+</sup> T cells in pre- or post-vaccination donors. **(F)** Alluvial plot showing the paired chain BCR gene usage of pre- or post-vaccination donors. **(G)** Full length amino sequence of TRAV23-DV6-TRAJ52-TRAC and TRBV7-6-TRBJ2-1-TRBC2.

instance, before vaccination, CD1C<sup>+</sup> aDC of both donors showed a high level of interaction with other types of cells. After vaccination, CD14<sup>+</sup> monocytes in both donors showed higher interaction levels with other type of cells. After vaccination, in both Donor 1 and Donor 2, CD8<sup>+</sup> T cells showed potential interaction with memory B via CD27-CD70, with CD16<sup>+</sup> monocytes via RIPK-TNF, ADRB2-IL1B and CCL4L2-FAR2, with CD1C<sup>+</sup> aDC via FAS-TNF, with CD14<sup>+</sup> monocytes via CD52-SIGLEC10, TNFRSF1A-TNF, ADRB2-IL1B, ITGaMb2-ICAM1, FAS-TNF, CD2-CD58 and LAIR1-LILRB4. These interactions were not detected pre-vaccination (Fig. 1G; Fig. S3B).

### Single-cell B and T cell receptor analysis of the vaccination candidates

To further explore the specific TCR or BCR enriched after vaccination, V and J regions gene usage of TRA (TCR $\alpha$ ) and TRB (TCR $\beta$ ) chains were analyzed by single-cell TCR and BCR sequencing assay (Fig. S4A). As illustrated in Figure 2A–D, TRAV23-DV6, TRAJ-52, TRBV7-6 and TRBJ2-1 showed the highest expression level in the post-vaccination group. Moreover, the percentages of these TCRs were significantly increased in comparison to the pre-vaccination group. To determine the paired chain TCR gene usage

corresponding to each cell type, the barcode of each cluster was imported to loupe vdj browser for single-cell level paired chain TCR gene usage analysis. Our data revealed an enrichment of a specific TCR clonal type in CD8<sup>+</sup> T cells expressing TRAV23-DV6-TRAJ52-TRBV7-6-TRBJ2-1 (Fig. 2E), while no enrichment of TCR sequence was observed in CD4<sup>+</sup> naïve T cell and CD4<sup>+</sup> Tcm (Fig. S4B, C). Surprisingly, no significant enrichment of clonotypes was observed in our BCR gene usage analysis, in both pre-vaccination and post-vaccination groups (Fig. 2F), probably due to the early-stage post-vaccination. The detailed amino acid sequence of highly enriched CD8<sup>+</sup> T clonotypes was provided in Figure 2G.

### Gene expression feature of the clonal CD8<sup>+</sup> T cells

To investigate the characteristic of the T-cells expressing TRAV23-DV6 and TRBV7-6, we projected these cells to tSNE map and analyzed their expression profile. Figure 3A and S5A demonstrated that these cells were enriched in CD8<sup>+</sup> cells in post-vaccination group and formed an independent cluster, suggesting that these cells may have distinct expression profiles among T cells. The barcodes of CD8<sup>+</sup> cells expressing TRAV23-DV6, TRAJ-52, TRBV7-6 and TRBJ2-1 (clonal CD8<sup>+</sup> T cells) were then extracted to generate a cell cluster for differentially expressed gene (DEG) analysis. To systematically investigate the unique gene expression pattern of this enriched T cell cluster, we conducted 3 comparisons from different aspects including clonal CD8<sup>+</sup> T cells vs. nonclonal CD8<sup>+</sup> T cells post-vaccination, nonclonal CD8<sup>+</sup> T cells post-vaccination vs. CD8<sup>+</sup> T cells pre-vaccination, clonal CD8<sup>+</sup> T cells post-vaccination vs. CD8<sup>+</sup> T cells pre-vaccination.

As shown in Figure S7, the top 50 upregulated genes in the clonal CD8<sup>+</sup> T cells vs. non-clonal CD8<sup>+</sup> T cells post-vaccination were illustrated in the heatmap (Fig. S7A, B). Next, KEGG analysis was performed to evaluate the pathway enrichment of the significantly upregulated genes. The enrichment of DEGs in the antigen presentation pathway was observed in both comparisons of clonal CD8<sup>+</sup> T cells vs. pre-vaccination CD8<sup>+</sup> T cells and clonal CD8<sup>+</sup> T cells vs. non-clonal CD8<sup>+</sup> T cells post-vaccination. Type-II HLAs including HLA-DPA1, HLA-DPB1 and HLA-DRB1 showed the highest expression level in the clonal CD8<sup>+</sup> T cells compared to other groups. Furthermore, HLA-I-based antigen presentation-related genes including CALR, TAP, HLA-I and HLA-II also showed high expression levels in the clonal CD8<sup>+</sup> T cells. These data suggest an intensive antigen presentation process occurring in these cells post-vaccination.

Interestingly, enrichment of DEGs in the phagosome pathway was also observed in the clonal CD8<sup>+</sup> T cells (Fig. 3B; Fig. S5B). Rab5 (a marker of early phagosome) and TUBA/TUBB (sub-unit forming the tubulin protein), LAMP2(lysosome marker), and vATPase (involved in the acidification of phagosome or phagolysosome) were highly expressed in the clonal CD8<sup>+</sup> T cells (Fig. S7C, D). Moreover, the granzyme family including GZMA, GZMB, and GZMH related to the cytotoxicity of CD8<sup>+</sup> T cells showed the highest expression level in the clonal CD8<sup>+</sup> T cells. In addition, a higher level of TNF and IFNG expression can also be observed in the clonal CD8<sup>+</sup> T cell (Fig. 3C). The DEGs

were then mapped to KEGG phagosome pathway (hsa04145). Fibrinogen receptors complex including ITGAM/ITGB2 (CR3), ITGA2/ITGB1, and ITGA5/ITGB1 were highly expressed in the clonal CD8<sup>+</sup> T cells. Together, these data suggest that this cluster of clonal CD8<sup>+</sup> T cells is equipped with vigorous cell killing activity, phagocytosis and antigen presentation functions.

### The cell–cell communication network of the clonal CD8<sup>+</sup> T cells

To further investigate the function of clonal CD8<sup>+</sup> T cells, we analyzed the cell–cell communication network of these clonal CD8<sup>+</sup> T cells with other cells using cellphonedb. Both donors exhibited a high level of interaction between clonal CD8<sup>+</sup> T cells and CD14<sup>+</sup> monocytes, CD16<sup>+</sup> monocytes and CD1C<sup>+</sup> aDC (Fig. 3D; Fig. S5C). The potential cell interactions of clonal CD8<sup>+</sup> T cells with CD14<sup>+</sup> monocytes, CD16<sup>+</sup> monocytes and CD1C<sup>+</sup> aDC are likely mediated by ICAM1-ITGAM/ITGB2 signaling pathway, revealing that these cells may potentially initiate the phagocytosis of this clonal CD8<sup>+</sup> T cells via ICAM1-ITGAM and ITGB2 signaling. When compared to other CD8<sup>+</sup> T cells in the post-vaccination group, the clonal CD8<sup>+</sup> T cells showed higher probability of interaction to CD14<sup>+</sup> monocytes and CD16<sup>+</sup> monocytes, likely via the CCL4-CCR5 pathway (Fig. 3E; Fig. S6E, S6F).

In both Donors, the clonal CD8<sup>+</sup> T cells showed potential interaction with memory B cells via IFNG- Type- II IFNR and TNFSF14-TNFRSF14 signaling; with CD16<sup>+</sup> monocytes via TNFSF14-TNFRSF14, ITGaMb2-ICAM1, TGFB3-TGFB1 and KLRF1-CLEC2B signaling; with CD1C<sup>+</sup> aDC via CD48-CD244, TNFRSF14-MIF and ITGaMb2-ICAM1 signaling; with CD14<sup>+</sup> monocytes via TNFSF14-TNFRSF14, ITGaMb2-ICAM1 and CCR5-CCL4 signaling post-vaccination. Notably, these interactions cannot be detected in nonclonal CD8<sup>+</sup> T cells (Fig. 3E; Fig. S6A, S6B). Furthermore, we compared the DEGs of CD14<sup>+</sup> monocytes, CD16<sup>+</sup> monocytes, CD1C<sup>+</sup> aDC and memory B cells pre- and post-vaccination. The up-regulation of NFKBIA, NFKBIZ, CCL3, IL1B, CXCL8, CCL3L1, CCL4L2 in CD14<sup>+</sup> monocytes; IL1B, CXCL8, TNF, CCL3 in CD16<sup>+</sup> Monocytes and CD1C<sup>+</sup>aDC; TNF, JUN, HLA- DQB1 in memory B cells were observed (Fig. 3F; Fig. S7E), which may facilitate cell–cell communication between these cells via these ligands.

### Clonotype abundance and gene usage in COVID-19 patients

Next, we further explored the diversity and enrichment of TCR clonotypes during SARS-CoV-2 infection. The quantification of unique clonotypes and gene usage analysis was performed on the PBMC from 36 healthy (H), 50 COVID-19 convalescent patients (C) and 6 COVID-19 dead patients (D). As shown in Figure 4A and B, there were around 60,000 unique TRA clonotypes and around 150,000 TRB clonotypes in the healthy controls group. In contrast, the dead and convalescent groups showed more concentrated TRA (~32,000 and ~30,000, respectively) and TRB clonotypes (~40,000 and ~60,000, respectively) distribution. The relative TRA and TRB clonotypes abundance analysis also

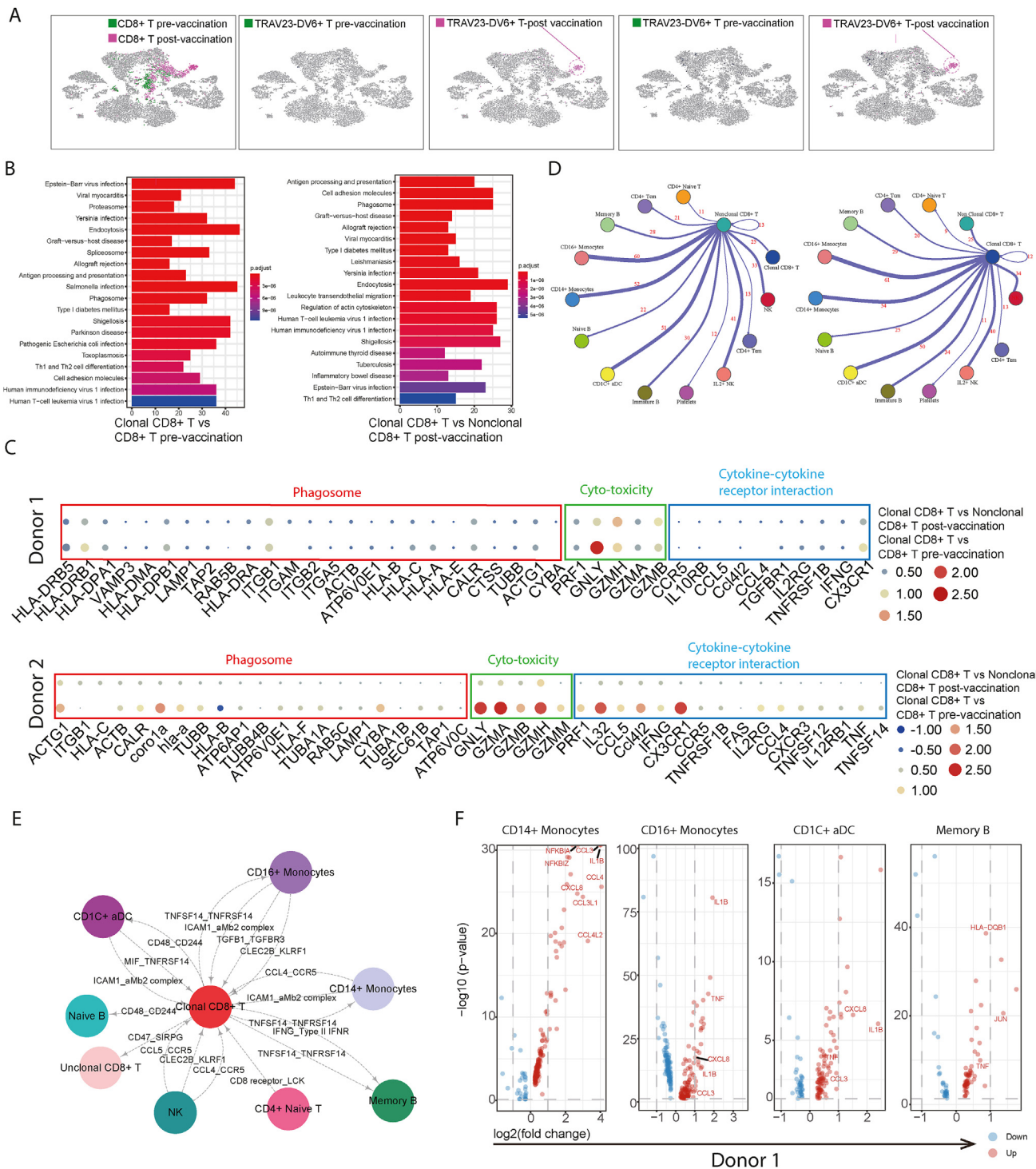


**Figure 3** Transcriptome characteristic of clonal  $CD8^+$  T cells. **(A)** tSNE plot mapping of TRAV23-DV6 and TRBV7-6 expression with the red filled dot indicating the clonal TCR positive T cells of Donor 1. **(B)** Bar plot of KEGG enrichment for the DEGs of the clonal  $CD8^+$  T cells vs. nonclonal  $CD8^+$  T cells post-vaccination in Donor 1; the clonal  $CD8^+$  T cells vs. total  $CD8^+$  T cells pre-vaccination with the color of the bar representing the adjusted  $P$  value and the height of the bar indicates the number of the genes enriched in the pathway. **(C)** Curved plot showing the number of interaction pair of post-vaccination  $CD8^+$  T cells and the clonal  $CD8^+$  T cells with other types of cells in Donor 1. **(D)** Heatmap illustrating the  $\log_2$  foldchange of phagosome, cyto-toxicity, cytokine and cytokine receptor related gene expression in the clonal  $CD8^+$  T cells vs. nonclonal  $CD8^+$  T Cells post-vaccination and the clonal  $CD8^+$  T cells vs. total  $CD8^+$  T cells pre-vaccination in both Donor 1 and Donor 2. **(E)** Clonal  $CD8^+$  T cells centered interaction network in both donors post-vaccination, with the molecular pairs in ligand (source cell) in left and receptor (target cell) in right. These interactions cannot be detected in nonclonal  $CD8^+$  T cells.

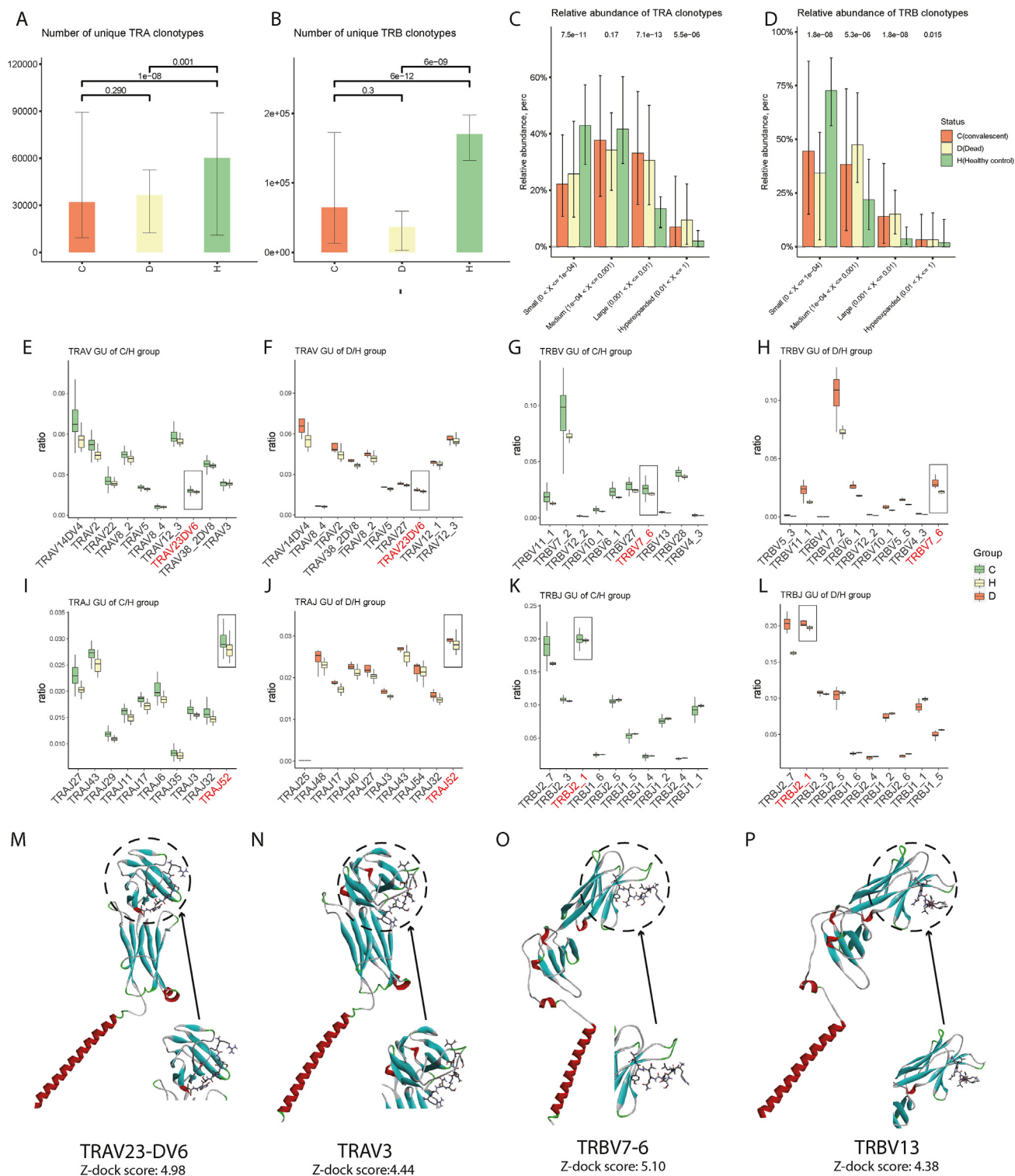


**Figure 4** TCR expansion in COVID-19 patients and healthy control. (A) Unique TCR A chain clonotypes quantification among groups. (B) Unique TCR B chain clonotypes quantification among groups. (C–F) TRAV gene usage ratio in C/H, D/H group. (G, H) TRBV gene usage ratio in C/H, D/H group. (I, J) TRAJ gene usage ratio in C/H, D/H group. (L, M) TRBJ gene usage ratio in C/H, D/H group. (N) *In-silico* docking of COVID-19 S1 epitope to homologue simulated TRAV23- DV6- TRAJ52- TRAC structure. (O) *In-silico* docking of SARS-CoV-2 S1 epitope to homologue simulated TRAV3- TRAJ17- TRAC structure. (P) *In-silico* docking of SARS-CoV-2 nucleocapsid epitope (yellow) to homologue simulated TRBV7-6- TRBJ2-1- TRBC2 structure. (Q) *In-silico* docking of SARS-CoV-2 nucleocapsid epitope (purple) to homologue simulated TRBV13- TRBJ2-3- TRBC2 structure. Statistical difference was measured with wilcox test,  $P$ -value  $< 0.05$  was considered statistically different.

revealed less TCR clonal expansion in healthy controls (Fig. 4C, D).

The specific recognition of antigen by TCR relies on the TCR sequence generated from the recombination of multiple clonotypes. To investigate the enriched clonotypes during SARS-CoV-2 infection, the gene usage analysis among different groups was performed by geneUsage function of immunarch. V and J regions of TRA and TRB were analyzed independently. The expression rate of each clonotype was firstly compared between convalescent patients and healthy control groups. Clonotypes including TRAV23DV6 for TRAV genes; TRAJ52 for TRAJ genes; TRBV7-6 for TRBV genes; TRBJ2-1 for TRBJ genes have a significantly higher percentage in total gene usage in convalescent patients than that of the healthy control. Notably, the higher ratio of TRAV23-DV6, TRAJ52, TRBV7-6 and TRBJ 2-1 could also be observed in the up-regulated clonotypes in the post-vaccination group (Fig. 4E–L).

Next, the potential interaction of these TCR candidates with the SARS-CoV-2 antigen was investigated by structure modeling. The full-length sequence of TRAV23-DV6-TRAJ52-TRBV7-6-TRBJ2-1 (the most enriched clonotype in the post-vaccination group) and TRAV3-TRAJ17-TRBV13-TRBJ2-3 (the clonotype has the lowest ratio in the post-vaccination group which was used as a control), were derived from the universal reference of vdj loupe browser, and then submitted to swiss model for structure simulation. It has been reported that the nucleocapsid of SARS-CoV-2 was an epitope for CD4<sup>+</sup> and CD8<sup>+</sup> T cells.<sup>21</sup> The structure of SARS-CoV-2 nucleocapsid epitope N105-113, was downloaded from RCSB PDB (<https://www.rcsb.org/structure/7LGD>) and *in-silico* docked with TRAV23- DV6- TRAJ52, TRBV7-6-TRBJ2-1, TRAV3-TRAJ17 and TRBV13- TRBJ2-3, respectively. The binding affinity was then estimated by Z-dock score, which suggested both TRAV23- DV6- TRAJ52 and TRBV7-6-TRBJ2-1 have a much higher affinity to nucleocapsid peptide than that of TRAV3-TRAJ17 and TRBV13- TRBJ2-3 (Fig. 4M–P).

## Discussion

Our study provided a landscape of the immune response after COVID-19 inactivated vaccine vaccination. However, only two samples were involved for single cell TCR and BCR sequencing, TCR clonotype enrichment was validated in 50 convalescent patients and 6 dead patients. We observed slightly more concentrated TCR enrichment in the COVID-19 patients compared to healthy control, which correlates with the single cell TCR sequencing study. Moreover, we also observed the enrichment of the same TCR identified by single-cell TCR sequencing in the patients, suggesting the reliability of these data.

Illumination of the adaptive immunity during SARS-CoV-2 vaccination and infection is crucial to the understanding of the pathogenesis of SARS-CoV-2 and may provide a theoretical basis for the therapy and prevention for COVID-19. Here we systematically delineated the detailed immunological response during SARS-CoV-2 vaccination and infection at the single-cell level. Our single transcriptome analysis revealed activation of different immunocyte types post-vaccination. The up-regulation of pro-inflammatory

cytokines including *IL1B*, *CCL3*, and *CXCL8* in CD14<sup>+</sup> monocytes was observed, which was constant with previous single-cell transcriptome studies of COVID-19 patients.<sup>3</sup> It has been shown that *CCL3* secreted by CD14<sup>+</sup> monocytes can recruit T cells and monocytes to the Antigen Presentation Cells, initiate the active antigen presentation and enhance CD8<sup>+</sup> T cells mediated cell killing activity.<sup>22</sup> Constantly, we found that TCR co-receptor subunit *CD8A* and *CD8B* which are involved in antigen presentation and the cytotoxicity gene *GNLY* were both up-regulated in CD8<sup>+</sup> T cells post-vaccination. These data suggested that, upon vaccination, CD14<sup>+</sup> monocytes may induce enhanced antigen presentation and cytotoxic activity of CD8<sup>+</sup> T cells, probably via *CCL3*.

During the immune response, the immunocytes undergo dynamic interaction with each other. Although several studies have demonstrated the immune response to SARS-CoV-2 at the single-cell transcriptome level, the transcription analysis-based cell–cell interactions network has been rarely reported. Our study revealed a distinct cell–cell interaction network upon vaccination, such as the potential interactions between CD14<sup>+</sup> monocytes and CD8<sup>+</sup> T cells via TNF- TNFRSF1A signaling post-vaccination. As TNF can activate the NF-κB signaling pathway through TNFRSF1A,<sup>23,24</sup> it may lead to the maturation of CD8<sup>+</sup> T cells. Moreover, we showed that CD8<sup>+</sup> T cells may interact with memory B cells by the CD27-CD70 pathway. It has been reported that CD70 can facilitate the activation and immunoglobin synthesis of B cells.<sup>25</sup> In line with this, our data demonstrate the increase of memory B cells post-vaccination. It would be of great interest to further investigate how these dynamic interactions regulate the activation and proliferation of the immunocytes during SARS-CoV-2 vaccination and infection.

A lot of studies indicated that CD4<sup>+</sup> T cells were the main participants in the virus infection. It has also been demonstrated that CD8<sup>+</sup> also facilitates the immune response to various viruses, including HIV,<sup>26</sup> influenza virus,<sup>27</sup> and SARS-CoV-2.<sup>28</sup> In our study, the samples were collected at the early phase post-vaccination (15 days post 2nd vaccination), CD8<sup>+</sup> T cells might be the first cells with clonotype enrichment. With the extension of the time after vaccination, the enrichment of BCR and TCR clonotypes on CD4<sup>+</sup> T cells might be observed.

While the humoral immune reaction is indispensable for adaptive immunity, the detailed T-cell response after SARS-CoV-2 vaccination and infection, especially at a single-cell level, was poorly characterized. The absence of significant BCR enrichment suggested that the T cells might dominate the adaptive immune responses in the early phase post-vaccination. By single-cell TCR-seq, we observed intense TCR clonotype TRAV23-DV6- TRAJ52, TRBV7-6 -TRBJ2-1, TRAV3 -TRAJ17 were significantly enriched in CD8<sup>+</sup> T cells post-vaccination. While we did not observe any clonotypes with a significant change between dead COVID-19 patients and convalescent COVID-19 patients (or individuals), healthy control groups, enriched clonotypes detected in single-cell sequencing also showed a significantly higher percentage in COVID-19 patients in comparison to the healthy controls. Notably, the TCR clonotype TRBV7-6 and TRBJ2-1 have also been identified with a higher percentage in COVID-19 patients in previous studies,<sup>29,30</sup> indicating the crucial role of

these TCR in SARS-CoV-2 clearance. Our molecular docking analysis also suggests a high interaction affinity of these TCR clonotypes with the epitope of nucleocapsid protein of SARS-CoV-2. delta SARS-CoV-2 shares the same protein sequence of the epitope with the current vaccine strain<sup>28</sup>. Moreover, the Omicron strain showed high sequence similarity with the vaccine strain on nucleocapsid coding region, implying this T-cell clonotype could be still effective in the protection of delta SARS-CoV-2. As CAR-T-based therapy has been applied to many virus infectious diseases including AIDS and EBV infection,<sup>12,31</sup> the identification of this TCR clonotype may facilitate the development of CAR-T therapy on COVID-19.

Our single-cell gene expression and cell–cell interaction analysis revealed the strong activities of phagocytosis and antigen presentation in the clonal CD8<sup>+</sup> T cells. While the phagocytosis function of CD4<sup>+</sup> T cells has been reported, it is not considered as the main function of T cells.<sup>32</sup> These data may uncover an uncanonical function of CD8<sup>+</sup> T cells. We hypothesized that these clonal CD8<sup>+</sup> T cells might be able to induce the apoptosis of SARS-CoV-2 containing cells and then engulf the debris with antigens. The antigen is subsequently processed and presented onto the HLA molecules, which could be recognized by other clonal CD8<sup>+</sup> T cells and induce the secretion of cytokines.

A recent COVID-19 vaccine study showed increasement in TNF and IFN- $\gamma$  secretion by CD4<sup>+</sup> T cells after vaccination.<sup>33</sup> Our single-cell expression analysis showed high expression of TNF and IFN- $\gamma$  post-vaccination in the clonal CD8<sup>+</sup> T cells. It has been shown that IFN- $\gamma$  promotes the synthesis of TNF and the high expression of IFN- $\gamma$  may induce extended TNF production in clonal CD8<sup>+</sup> T cells in a self-activation manner. Moreover, TNF has been reported to stimulate the secretion of IL-1B and CXCL8 in monocytes.<sup>34</sup> Our single-cell expression profile and cell–cell interaction data suggested that the higher expression of IL-1B and CXCL8 by CD14<sup>+</sup> monocytes post-vaccination may be due to the extended secretion of TNF by clonal CD8<sup>+</sup> T cells.

According to another single-cell sequencing study of mRNA vaccine<sup>35</sup> which collect the sample at a similar time point as our study (2 weeks after 2nd vaccination). This study showed a different TCR enrichment post-vaccination, while the TCR enrichment can be observed in both CD4<sup>+</sup> and CD8<sup>+</sup> T cells and BCR clonotype enrichment can be observed in B cells. Considering the instruction of inactivated vaccine that antibody could be detected 1 month after 2nd vaccination. This might indicate that the mRNA vaccine might induce a more rapid immune response than the inactivated vaccine. This study also highlights diverse TCR clonotype enrichment in patients, while this phenomenon can also be observed in our study, this might be due to the different epitope presentation processes in different individuals. Compared to the patients, vaccine candidates showed a more concentrated TCR clonotype enrichment. Another study also highlights a fully functional CD8<sup>+</sup> T cell response from one week after the first bnt162b2 vaccine, while CD4<sup>+</sup> T cell response and B cell response were hardly detectable. Indicating earlier activation of CD8<sup>+</sup> T cells.<sup>36</sup>

The profiling of TCR enrichment might facilitate the development of CAR-T therapy against COVID-19. The CAR-T cell contains a TCR to target the cells expressing a specific

epitope, which enables the CAR-T cells to eliminate target cells. Currently, CAR-T has been widely used to treat various tumors, but it could also be applied to treat diseases caused by intracellular pathogens including bacteria and viruses. The identification of SARS-CoV-2 specific TCR may contribute to engineering CAR-T cells to eliminate SARS-CoV-2 infected target cells for future studies.

## Conclusion

Together, we delineated the single-cell transcriptome landscape and TCR dynamic of inactivated SARS-CoV-2 vaccination candidates. The specific TCR enrichment has also been identified in the COVID-19 vaccination candidates. Our data revealed a robust clonal CD8<sup>+</sup> T cell immune response and uncovered an uncanonical phagocytosis activity and antigen presentation function of the clonal CD8<sup>+</sup> T cells post-vaccination. It could provide a better understanding of the immunological response during SARS-CoV-2 vaccination/infection and thus facilitate the development of T-cell-based therapy against COVID-19.

## Code availability

The code for processing single-cell RNA-seq data and bulk TCR data is available at <https://github.com/MSN-06s/scRNA-seq/tree/main>.

## Ethics declaration

The vaccination study has been approved by the ethics committee of Maternal and Child Health Hospital of Hubei, Wuhan, China with the approval number LW018. The patient study has been approved by the ethics committee of General Hospital of Central Theater Command with the approval number [2022] 011-1.

## Consent for publication

All the authors and participants approve the publication of this paper.

## Author contributions

Xiaojian Cao and Keji Yan developed the methodology and construct the NGS library, Xiaohua Chen and Yaqi Zhu completed the sample collection and RNA isolation for bulk TCR libraries construction, Xiaojian Cao and Xiaojuan Gou conducted the NGS data analysis, Bing Yang conducted the in-silico docking, Gang Cao, Xiaohua Chen and Yong-an Zhong supervised the project, Gang Cao designed the experiments and analysis. All authors contributed to the figure arrangement and manuscript writing and correction.

## Conflict of interests

All authors declared no conflict of interests.

## Funding

This work is funded by the National Natural Science Foundation of China (No. 31941014 to G.C), the Key Research and Development Program of Guangdong Province (No. 2019B020211003 to G.C.) and Fundamental Research Funds for the Central Universities (No. 2662018PY025 to G.C.).

## Data availability

The bulk TCR sequencing raw data files were deposited at the GSA of the human session of the National Genomics Data Center under the accession number HRA001115. The single-cell transcriptome and vdj sequencing raw data files were deposited at the GSA for the human session of the National Genomics Data Center under the accession number HRA001099.

## Appendix A. Supplementary data

Supplementary data to this article can be found online at <https://doi.org/10.1016/j.gendis.2022.08.020>.

## References

1. Cox RJ, Brokstad KA. Not just antibodies: B cells and T cells mediate immunity to COVID-19. *Nat Rev Immunol*. 2020;20(10):581–582.
2. Iwasaki A, Yang Y. The potential danger of suboptimal antibody responses in COVID-19. *Nat Rev Immunol*. 2020;20(6):339–341.
3. Wen W, Su W, Tang H, et al. Immune cell profiling of COVID-19 patients in the recovery stage by single-cell sequencing. *Cell Discov*. 2020;6:31.
4. Wilk AJ, Rustagi A, Zhao NQ, et al. A single-cell atlas of the peripheral immune response in patients with severe COVID-19. *Nat Med*. 2020;26(7):1070–1076.
5. Wang P, Jin X, Zhou W, et al. Comprehensive analysis of TCR repertoire in COVID-19 using single cell sequencing. *Genomics*. 2021;113(2):456–462.
6. Cañete PF, Vinuesa CG. COVID-19 makes B cells forget, but T cells remember. *Cell*. 2020;183(1):13–15.
7. Vabret N, Britton GJ, Gruber C, et al. Immunology of COVID-19: current state of the science. *Immunity*. 2020;52(6):910–941.
8. Alcover A, Alarcón B, di Bartolo V. Cell biology of T cell receptor expression and regulation. *Annu Rev Immunol*. 2018;36:103–125.
9. Rothenberg EV. Programming for T-lymphocyte fates: modularity and mechanisms. *Genes Dev*. 2019;33(17–18):1117–1135.
10. Davis MM, Boniface JJ, Reich Z, et al. Ligand recognition by alpha beta T cell receptors. *Annu Rev Immunol*. 1998;16:523–544.
11. Chiffelle J, Genolet R, Perez MA, Coukos G, Zoete V, Harari A. T-cell repertoire analysis and metrics of diversity and clonality. *Curr Opin Biotechnol*. 2020;65:284–295.
12. Namdari H, Rezaei F, Teymoori-Rad M, Mortezagholi S, Sadeghi A, Akbari A. CAR T cells: living HIV drugs. *Rev Med Virol*. 2020;30(6):1–14.
13. Bolotin DA, Poslavsky S, Mitrophanov I, et al. MiXCR: software for comprehensive adaptive immunity profiling. *Nat Methods*. 2015;12(5):380–381.
14. Hao Y, Hao S, Andersen-Nissen E, et al. Integrated analysis of multimodal single-cell data. *Cell*. 2021;184(13):3573–3587.
15. Aran D, Looney AP, Liu L, et al. Reference-based analysis of lung single-cell sequencing reveals a transitional profibrotic macrophage. *Nat Immunol*. 2019;20(2):163–172.
16. Efremova M, Vento-Tormo M, Teichmann SA, Vento-Tormo R. CellPhoneDB: inferring cell-cell communication from combined expression of multi-subunit ligand-receptor complexes. *Nat Protoc*. 2020;15(4):1484–1506.
17. Chen C, Chen H, Zhang Y, et al. TBtools: an integrative toolkit developed for interactive analyses of big biological data. *Mol Plant*. 2020;13(8):1194–1202.
18. Yu G, Wang LG, Han Y, He QY. clusterProfiler: an R package for comparing biological themes among gene clusters. *OMICS*. 2012;16(5):284–287.
19. Luo W, Brouwer C. Pathview: an R/Bioconductor package for pathway-based data integration and visualization. *Bioinformatics*. 2013;29(14):1830–1831.
20. Shannon P, Markiel A, Ozier O, et al. Cytoscape: a software environment for integrated models of biomolecular interaction networks. *Genome Res*. 2003;13(11):2498–2504.
21. Le Bert N, Tan AT, Kunasegaran K, et al. SARS-CoV-2-specific T cell immunity in cases of COVID-19 and SARS, and uninfected controls. *Nature*. 2020;584(7821):457–462.
22. Cook DN. The role of MIP-1 alpha in inflammation and hematopoiesis. *J Leukoc Biol*. 1996;59(1):61–66.
23. Lucas PC, McAllister-Lucas LM, Nunez G. NF-kappaB signaling in lymphocytes: a new cast of characters. *J Cell Sci*. 2004;117(Pt 1):31–39.
24. Webb LV, Ley SC, Seddon B. TNF activation of NF- $\kappa$ B is essential for development of single-positive thymocytes. *J Exp Med*. 2016;213(8):1399–1407.
25. Borst J, Hendriks J, Xiao Y. CD27 and CD70 in T cell and B cell activation. *Curr Opin Immunol*. 2005;17(3):275–281.
26. Freel SA, Saunders KO, Tomaras GD. CD8(+)T-cell-mediated control of HIV-1 and SIV infection. *Immunol Res*. 2011;49(1–3):135–146.
27. Jiang J, Fisher EM, Murasko DM. CD8 T cell responses to influenza virus infection in aged mice. *Ageing Res Rev*. 2011;10(4):422–427.
28. Lineburg KE, Grant EJ, Swaminathan S, et al. CD8 + T cells specific for an immunodominant SARS-CoV-2 nucleocapsid epitope cross-react with selective seasonal coronaviruses. *Immunity*. 2021;54(5):1055–1065.
29. Schultheiß C, Paschold L, Simnica D, et al. Next-generation sequencing of T and B cell receptor repertoires from COVID-19 patients showed signatures associated with severity of disease. *Immunity*. 2020;53(2):442–455.
30. Zhang JY, Wang XM, Xing X, et al. Single-cell landscape of immunological responses in patients with COVID-19. *Nat Immunol*. 2020;21(9):1107–1118.
31. Slabik C, Kalbanczyk M, Danisch S, et al. CAR-T cells targeting Epstein-Barr virus gp350 validated in a humanized mouse model of EBV infection and lymphoproliferative disease. *Mol Ther Oncolytics*. 2020;18:504–524.
32. Murphy S, Sylwester A, Kennedy RC, Soll DR. Phagocytosis of individual CD4+ T cells by HIV-induced T cell syncytia. *AIDS Res Hum Retroviruses*. 1995;11(4):433–442.
33. Ewer KJ, Barrett JR, Belij-Rammerstorfer S, et al. T cell and antibody responses induced by a single dose of ChAdOx1 nCoV-19 (AZD1222) vaccine in a phase 1/2 clinical trial. *Nat Med*. 2021;27(2):270–278.
34. Taniguchi-Ponciano K, Vadillo E, Mayani H, et al. Increased expression of hypoxia-induced factor 1 $\alpha$  mRNA and its related genes in myeloid blood cells from critically ill COVID-19 patients. *Ann Med*. 2021;53(1):197–207.
35. Sureshchandra S, Lewis SA, Doratt BM, Jankeel A, Coimbra Ibrahim I, Messaoudi I. Single-cell profiling of T and B cell repertoires following SARS-CoV-2 mRNA vaccine. *JCI Insight*. 2021;6(24):e153201.
36. Oberhardt V, Luxenburger H, Kemming J, et al. Rapid and stable mobilization of CD8(+) T cells by SARS-CoV-2 mRNA vaccine. *Nature*. 2021;597(7875):268–273.